Superconducting Resonators and Their Applications in Quantum Engineering

Nov. 2009

Lin Tian
University of California, Merced & KITP

Collaborators:
Kurt Jacobs (U Mass, Boston)
Raymond Simmonds (Boulder)
Hailin Wang (U Oregon)

Group:
Yong Hu (postdoc)
Dan Hu (student)
Xiuhao Deng (student)
Jon Inouye (student)

Support:
NSF, UCM-GRC

Solid-state devices, quantum information, and quantum effects

- Superconducting devices: flux qubit, charge qubit, phase qubit, stripeline resonator, lumped element LC
- Semiconductor systems: gated quantum dots, Si-based, NV centers, self-assembled dots, nanocavities
- Nanomechanical resonators: beam, cantilever, nanotube, microdisk
- Many other systems:
  exotic systems such as electrons on liquid helium ...

Artificial/Macroscopic atoms and oscillators can now be achieved
Better quantum engineering, control, and probing wanted

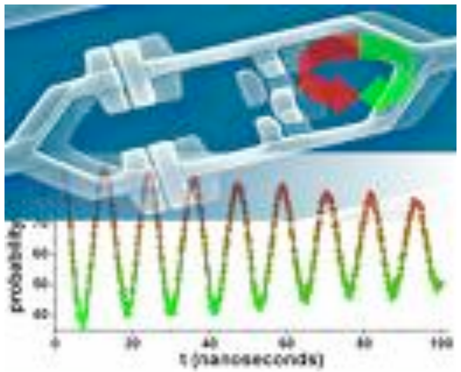

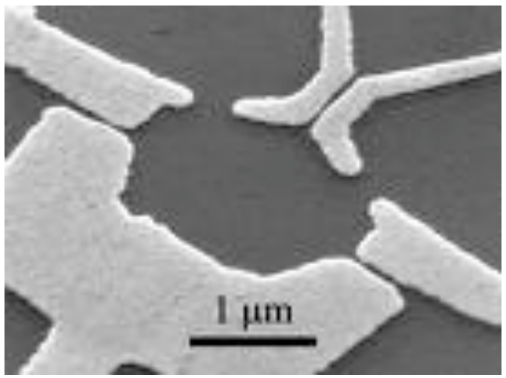

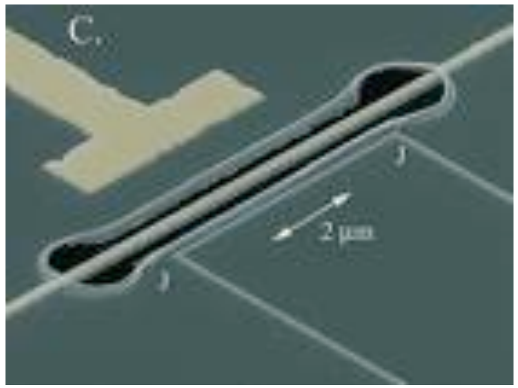

Beyond quantum computing and quantum information

- Quantum effect as a probe for microscopic effects in various solid-state devices

- Engineering to approach the quantum limit

- Novel many-body physics

Superconducting devices

Superconducting Qubits

Josephson junction

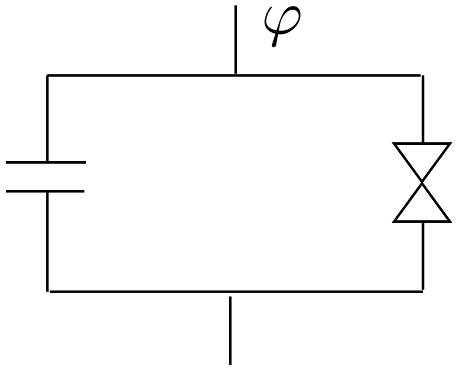

Charging Energy

$$\frac{m_\varphi}{2}\dot{\varphi}^2$$

Josephson Energy

$$-I_c\frac{\hbar}{2e}\cos\varphi$$

Quantum Hamiltonian

$$E_c = \frac{e^2}{2C} \qquad E_J = I_c\frac{\hbar}{2e}$$

Tunable E_J

$$H = \frac{\hat{P}_\varphi^2}{2m_\varphi} - I_c\frac{\hbar}{2e}\cos\varphi$$

$$\hat{P}_\varphi = -i\hbar\frac{\partial}{\partial\varphi} \qquad m_\varphi = C\left(\frac{\hbar}{2e}\right)^2$$

Various qubits have been tested with coherence time > μs
Josephson junction resonator has been tested $Q \sim 10^{3\text{-}4}$.

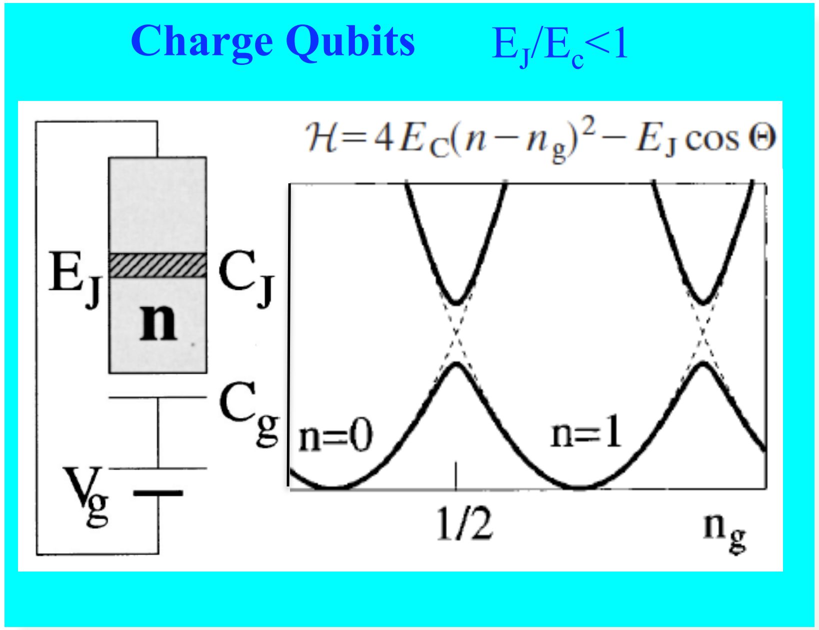

Flux qubit – Mooij, Orlando …
Charge qubit – Nakamura …
Phase qubit – Martinis …
Transmon – Schoelkopf, Girvin …
Other variation …

Makhlin, Schoen, Shnirman, 2002
Devoret, Wallraff, Martinis, 2004

Ion trap quantum computing

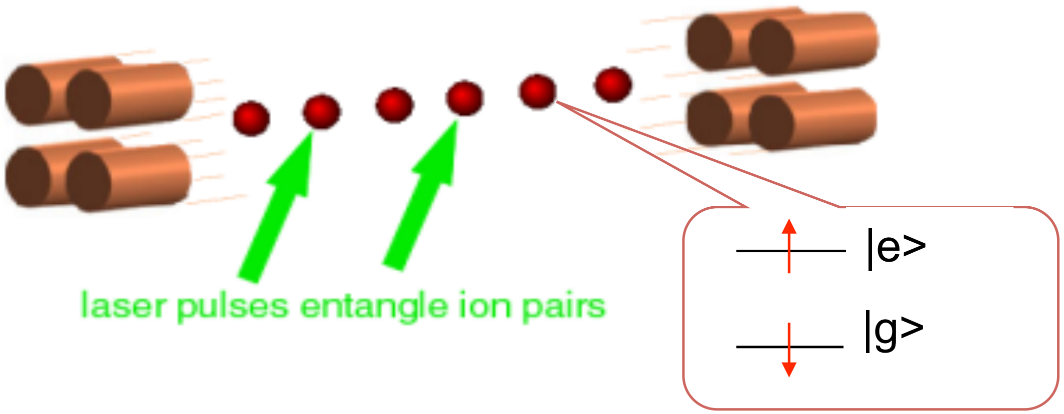

Cirac, Zoller, PRL (1995)

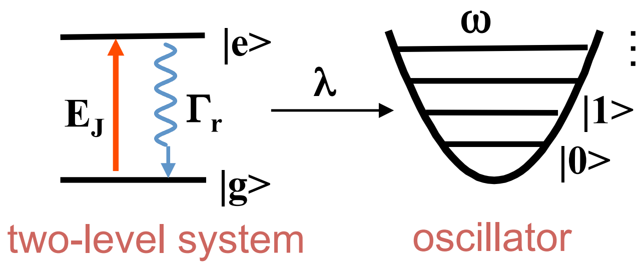

Harmonic motion as data bus mediating
Controlled quantum logic gates

Superconducting Resonators

Josephson junction resonator

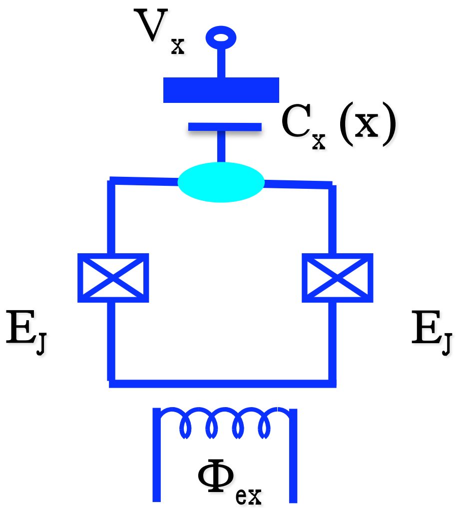

$$\frac{m_\varphi}{2}\dot{\varphi}^2$$
$$-I_c\frac{\hbar}{2e}\cos\varphi$$

Transmission line resonator

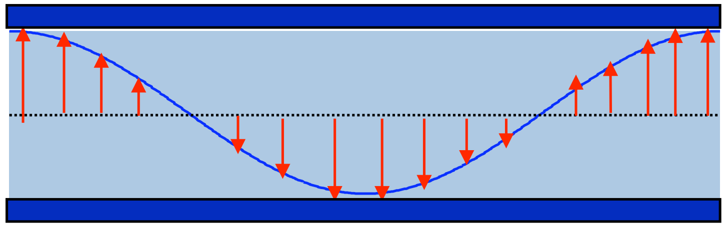

$$\mathcal{L} = \sum_k \frac{l}{2}\dot{\phi}_k^2 - \frac{1}{2c}\left(\frac{k\pi}{L}\right)^2\phi_k^2$$

$$\hat{\phi}_k(t) = \sqrt{\frac{\hbar\omega_k c}{2}}\frac{L}{k\pi}[a_k(t) + a_k^\dagger(t)]$$

- Q-factor ~$10^{3\text{-}7}$, can have long coherence time, Q controllable
- frequency GHz - tunable by external flux, external circuit (e.g. SQUID)
- strong coupling with qubits has been tested experimentally – Stark shift, Rabi splitting, Lamb shift, ……

Quantum Oscillators

Quantum resonator modes in nanoscale
- motional states in ion traps
- Josephson junction resonators
- superconducting transmission line
- nanomechanical modes

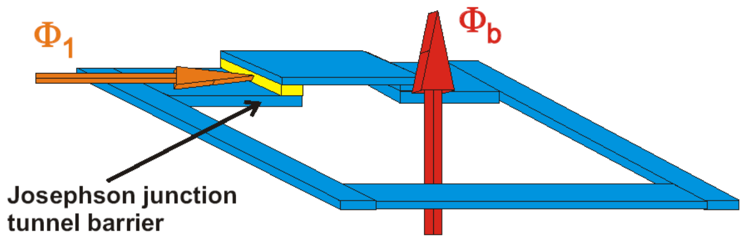

Smaller & more coherent (macroscopic) systems in their quantum limit!

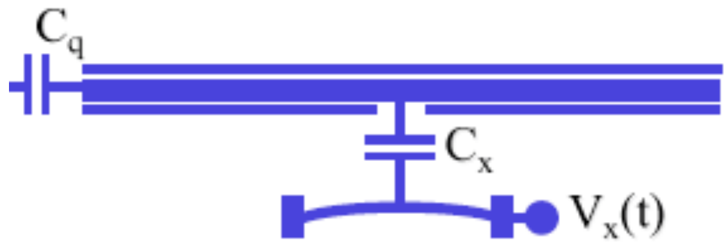

Transmission line

Quantum applications – Quantum information,

Metrology, foundations of quantum physics

…

Nanomechanical systems

Superconducting Resonators

- Progress – coherence & coupling
- Quantum engineering on TLS's – JJ resonator
- Novel many-body effects

Resonators vs TLS Flctuators

- Previous phase qubit measurements show spectroscopic splittings due to amorphous two-level system (TLS) fluctuators inside Josephson junctions (a strong source of decoherence). (Simmonds et al. 2004, Martinis et al. 2005, Neeley et al 2008, Y. Yu et al, 2008)

- Can we find a way to distinguish the coupling mechanism between the two-level systems (TLS) and the junction?, e.g. coupling to critical current or coupling to dielectric field.

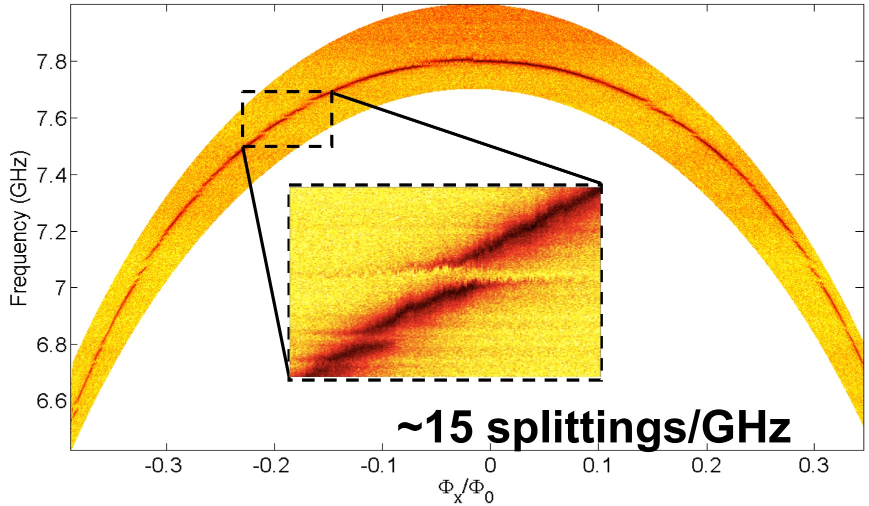

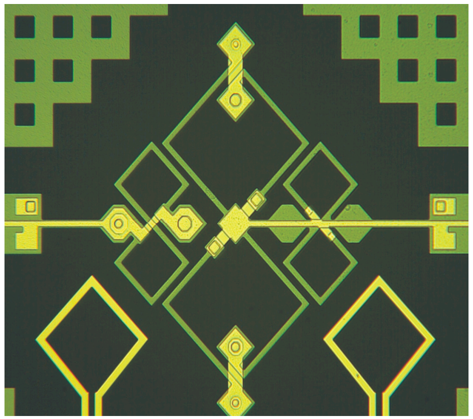

Cavity QED

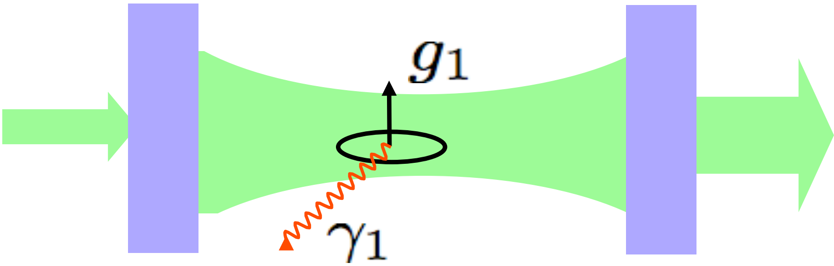

- atoms, ions in cavity
- quantum dot photonic devices
- superconducting quantum circuit

$$\hbar\omega_c \hat{a}^\dagger \hat{a} + \hbar\omega_1 \sigma_{1z} + g_1(\hat{a}\sigma_{1+} + \hat{a}^\dagger\sigma_{1-}) + \epsilon(\hat{a} + \hat{a}^\dagger) + H_\kappa + H_\gamma$$

- $\hbar\omega_c \hat{a}^\dagger \hat{a}$ → cavity - Josesphon junction resonator
- $\hbar\omega_1 \sigma_{1z}$ → atom – qubit (TLS)
- $g_1(\hat{a}\sigma_{1+} + \hat{a}^\dagger\sigma_{1-})$ → coupling
- $\epsilon(\hat{a} + \hat{a}^\dagger)$ → microwave driving
- H_κ → cavity damping
- H_γ → TLS noise

Δ_c - detuning of microwave mode
Δ_a - detuning of qubit (TLS)
g_1 - coupling, $g_1 = g_c$, g_d

Cavity QED in solid-state devices

- qubit
- TLS
- many-body Hamiltonian

Junction as Microscope for TLS

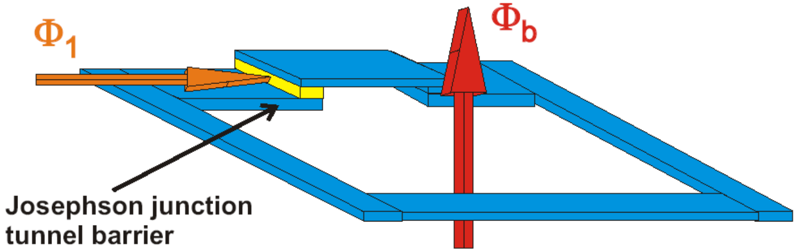

Tunable cavity frequency by adjusting Φ_b

1. frequency can scan through TLSs
2. frequency can be compensated to a fixed value when adjusting Φ_1

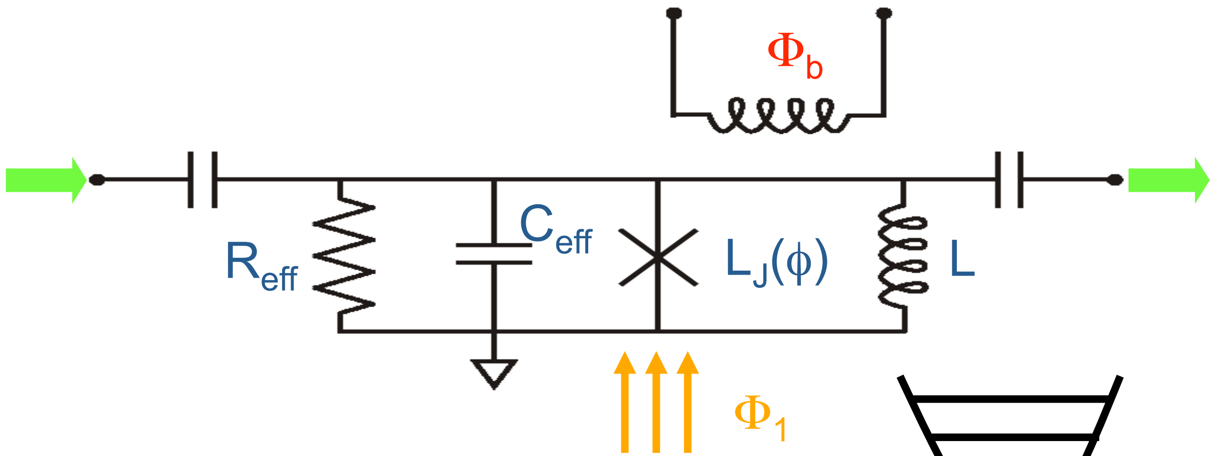

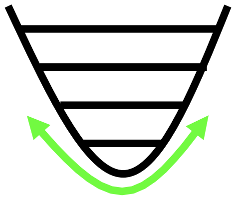

- using microwave transmission as microscope output
- using variable external field as a ruler to decide position/coupling of TLS
- interpret coupling mechanism by varying external field

Apply a Magnetic Field through the Junction Barrier

This creates a spatial modulation of the Josephson energy and the coupling with TLSs

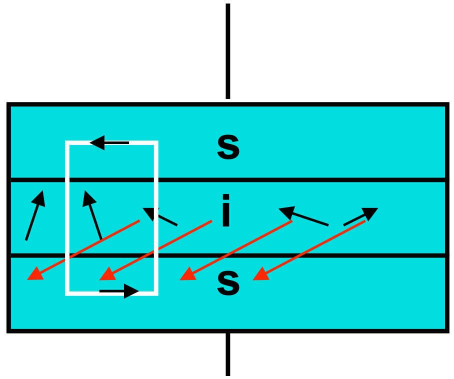

- Phase variable: $\varphi(r) = \varphi(0) + \frac{2e}{\hbar} B.A$
- Josephson energy: $-\frac{E_J}{L}\int_0^L dr \cos(\varphi + \lambda r)$
- Only critical current coupling should change with field

Critical Current Coupling

$$-E_{J1}\int_0^L dx \cos(\varphi + \varphi_1 \frac{x}{L})\vec{j}_d \cdot \vec{\sigma} f(x - r_d)$$

$$g_d = E_{J1} j_x \sqrt{\frac{2e^2}{C_J \hbar\omega_c}} \sin\varphi_1 (\frac{r_d}{L} - \frac{1}{2})$$

Dielectric coupling

$$-\frac{2e^2 d_0}{C_J h_0}\frac{\hat{p}_\varphi}{\hbar}$$

$$g_c = \frac{d_0}{h_0}\sqrt{\frac{e^2\hbar\omega_c}{2C}}$$

$\varphi_1 = \Phi_1/\Phi_0$ φ_1: total flux in junction

d_0: dipole, h_0: barrier thickness

Fluctuation of the Junction Transmission

Fluctuation of the junction transmission is directly related to fluctuation of TLS under the effective Bloch equation, and provides useful information about spectrum, decay, spatial information of the TLS

$$\widetilde{F}_{\sigma_-\sigma_+}(\omega) = F_{XX}(\omega)(\kappa^2 + (\omega - \Delta_c)^2)/g_1^2$$

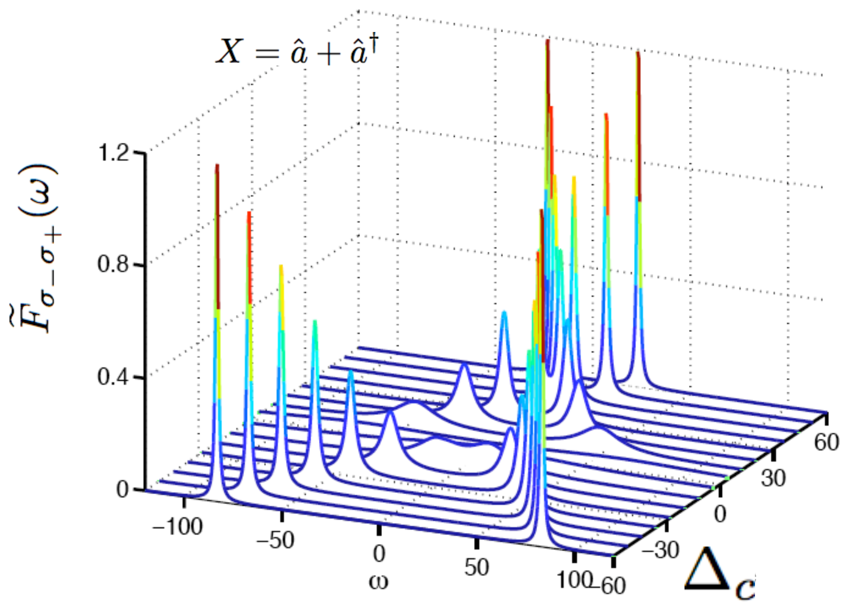

$\Delta_{ac} = 30$ MHz

Tian, Simmonds, PRL (2007)

- $\widetilde{F}_{\sigma_-\sigma_+}(\omega)$ dominated by Lorentzian terms of TLS with peaks at $\omega_p^{(1,2)} \approx \pm\Delta$

$$\longrightarrow \Delta_a - \frac{g^2\Delta_c}{\kappa^2 + \Delta_c^2}$$

- can be used to study coupling dependence, coherence of TLS, energy, and spatial distribution of TLS

Junction as **Coupler** for TLS Qubits

Possible long coherence time:

- (de)coherece time > than qubit

TLS's in the same junction

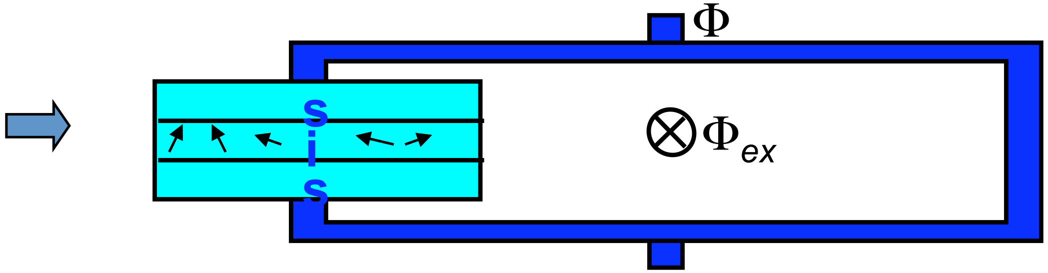

TLS in different junctions

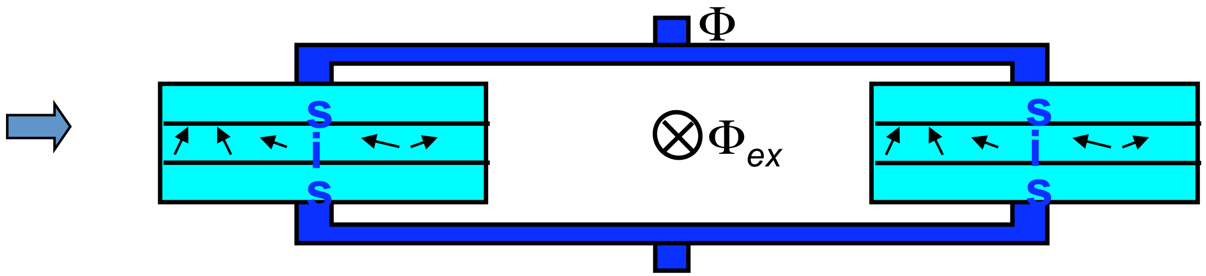

- Resonator as cavity to manipulate TLS's with large energy separation
- Universal quantum logic gates can be achieved via cavity
- Gates can reach high fidelity

$$\widetilde{H}_1 = \sum \frac{\bar{\Delta}_n}{2}\sigma_{nz} + \Omega_n \sigma_+ + \Omega_n^\star \sigma_- + \sum_{\langle n,m\rangle} \lambda_{nm}\sigma_{n+}\sigma_{m-} + \lambda_{nm}^\star \sigma_{m+}\sigma_{n-}$$

Two-Qubit Gate

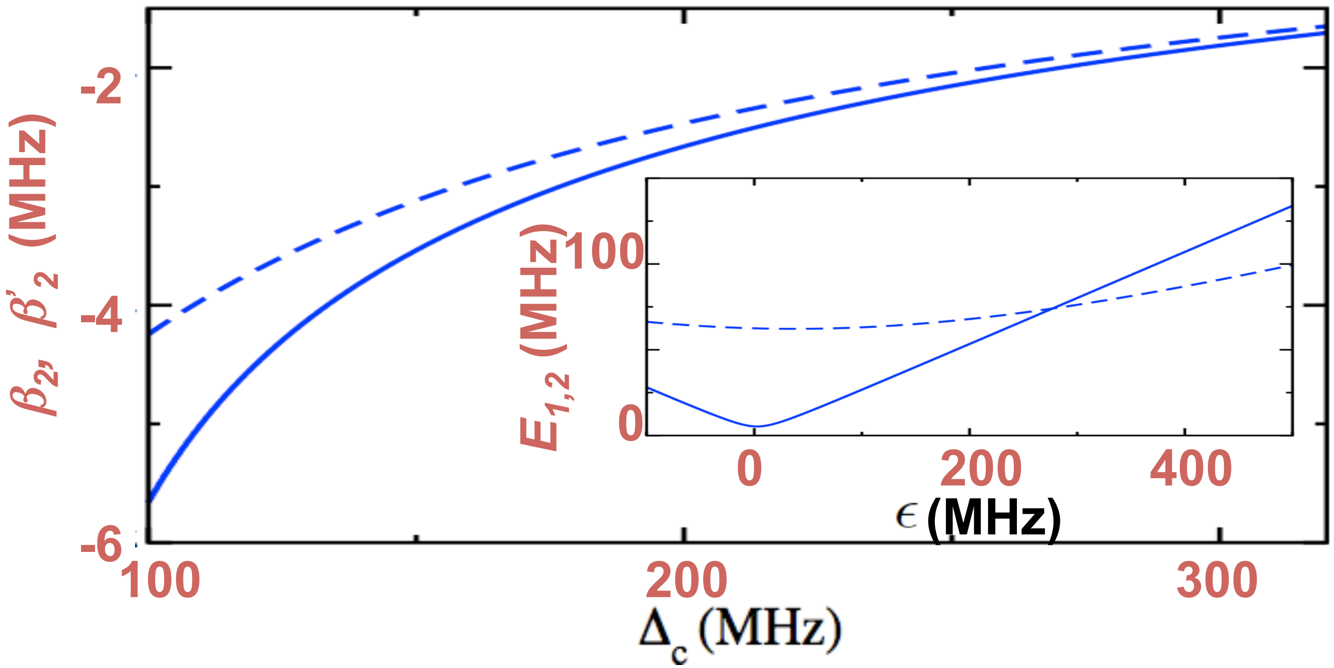

- TLS's are usually off-resonance; coupling can't implement gates
- Adjusting resonator to tune to resonance so that E_1=E_2 (inset)
- β_2' is effective coupling parameter including residuce coupling
- Two-bit gates can be performed in 150 ns.

Tian, Jacobs, PRB (2009)

CQED for Qubit Arrays

Josephson junction arrays have been studied for many-body physics
- classical JJA – two-dimensional XY, observe BKT transition
- quantum JJA – superconductor-Mott insulator transition
- quantum phase model
- dissipative quantum phase transition

2D array of JJ
$E_J >> E_c$ superconducting
$E_J << E_c$ Mott insulator

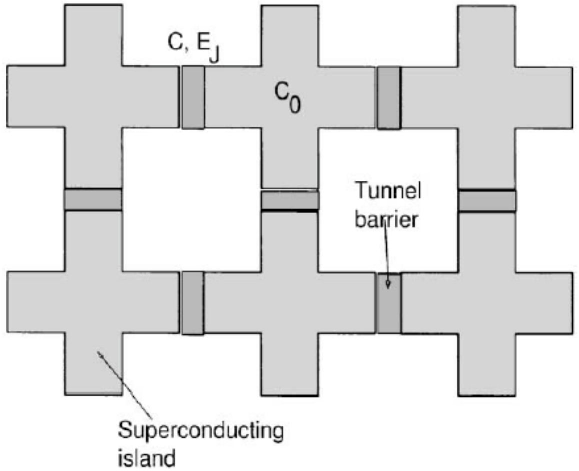

Recent progress in superconducting qubits brings more ……
- high-Q cavity mode
- strong coupling between qubits and cavity
- using cavity to measure qubits

CQED for Qubit Arrays

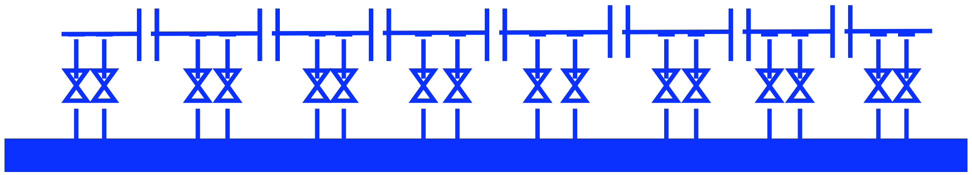

Qubit chain – define qubits at even/odd sites in opposite directions – NNN term

Quantum Ising model $H_0 = -J_x \sum_i \sigma_{xi} - \sum_i \sigma_{zi}\sigma_{zi+1}$

Resonator cavity – lumped element capacitance with loop inductance, driving detuning Δ_c

$$H_c = \hbar\omega_c a^\dagger a + \epsilon(t)(a + a^\dagger)$$

Coupling – magnetic field modulating effective inductance of cavity

Coupling $$H_{int} = g a^\dagger a \sum(\sigma_{xi})$$

Quantum Ising model

$$H_0 = -J_x \sum_i \sigma_{xi} - \sum_i \sigma_{zi}\sigma_{zi+1}$$

Small J_x, ferromagnetic states $|\uparrow \cdots \uparrow\rangle$ and $|\downarrow \cdots \downarrow\rangle$
Large J_x, paramagnetic states $|+ \cdots +\rangle$

Ground state average
(not standard order parameter)

$$X = \langle g|\sum \sigma_{xi}|g\rangle = \begin{cases} N, & J_x \gg 1 \\ 0, & J_x \ll 1 \end{cases}$$

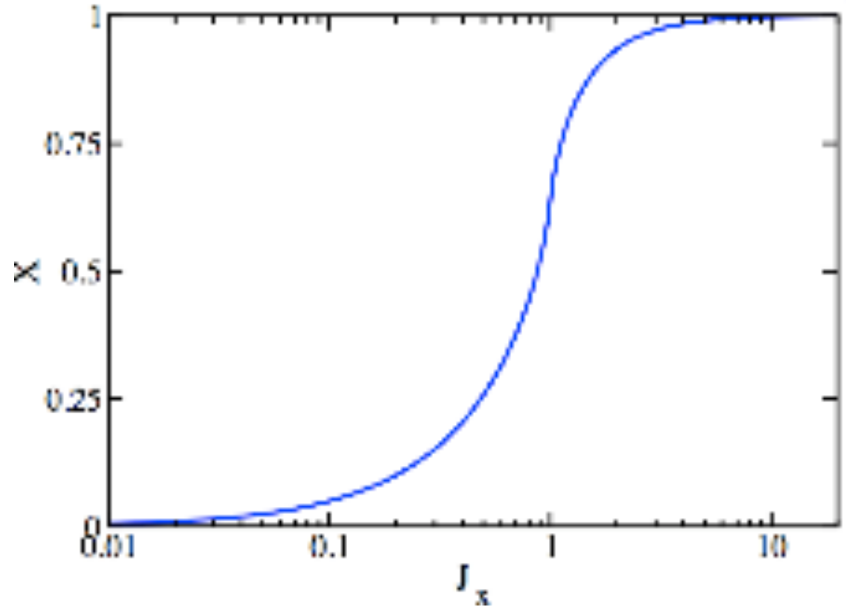

Nonlinear effect in cavity

Cavity photon number and many-body state;   Transversal field on photon number

$$n_{ss} = \frac{i\epsilon}{\kappa}\langle a - a^{\dagger}\rangle_{ss} = \frac{\epsilon^2}{\kappa^2/4 + (\Delta_c - gX)^2} \qquad \widetilde{J}_x = J_x - g n_{ss}$$

Fixed parameter $J_x > J_c=1$, $\Delta_c=0$

Driving increases – jump from lower branch to higher branch

• Weak driving: detection of many-body states

• Strong driving: bistable regime due to cavity nonlinear effect

Can be studied with just two qubits

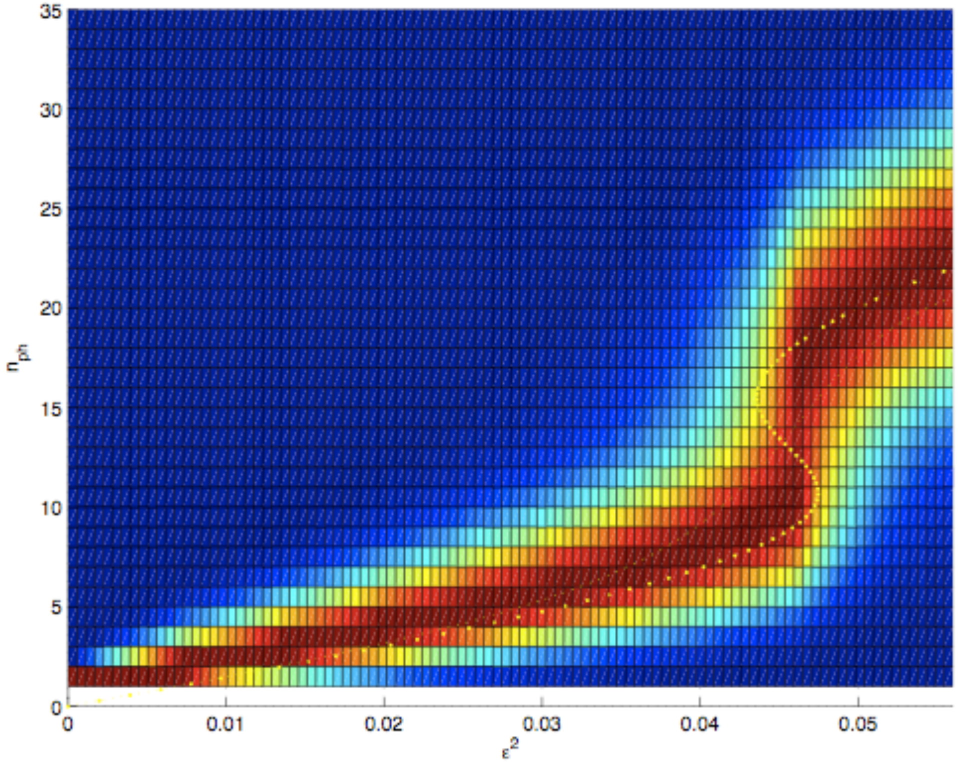

L. Tian, in preparation (2009)

Bistable regime and quantum fluctuations

Phase diagram by semiclassical approach

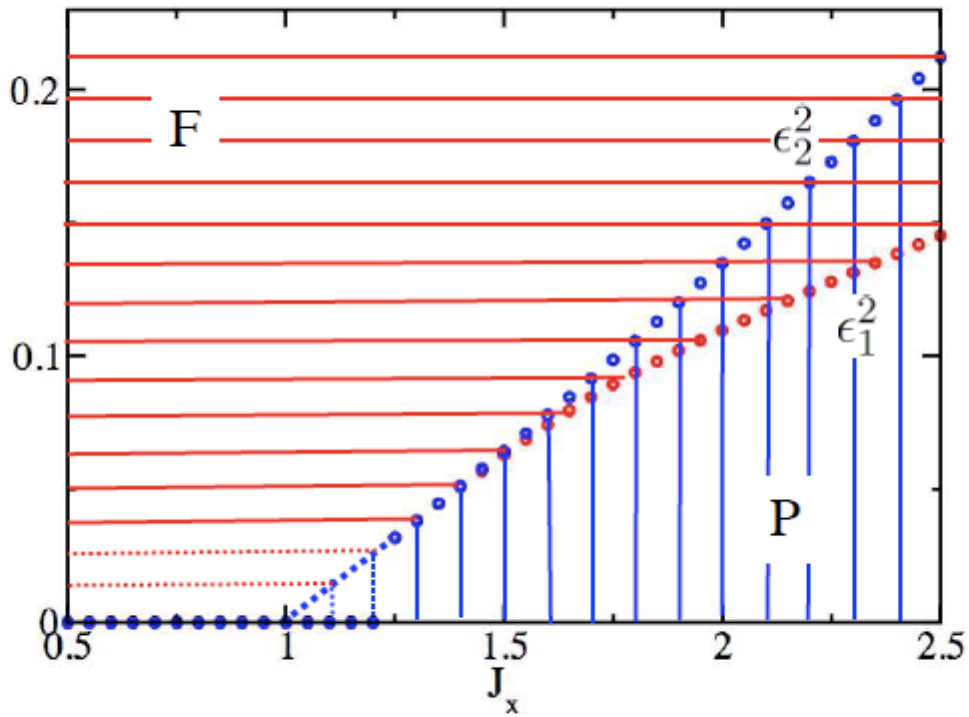

Semiclassical: nonlinear effect induces bistable regime for Ising model
Property of many-body state – affected strongly by quantum fluctuation
Entanglement reaches maximal near transition point

On-Demand Entangled Photon Pair

Effective Kerr-like interaction for resonator mode

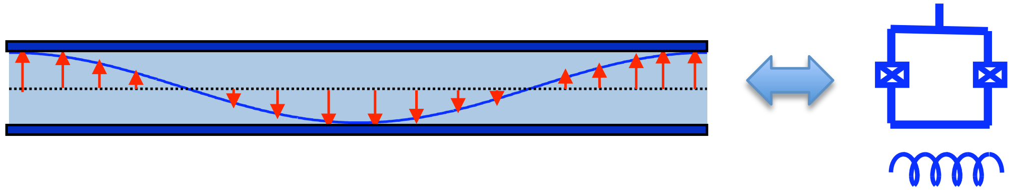

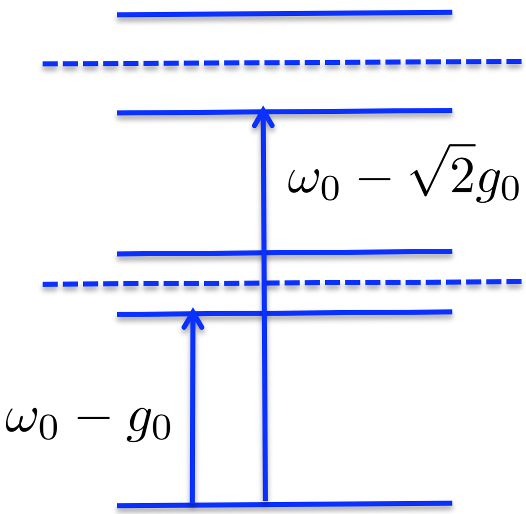

$$g_0(a^\dagger \sigma_- + \sigma_+ a)$$

$$\frac{U}{2} a^\dagger a^\dagger a a$$

Coupled resonators

$$H_{eff} = -t\sum a_i^\dagger a_{i+1} + \frac{U}{2}\sum a_i^\dagger a_i^\dagger a_i a_i$$

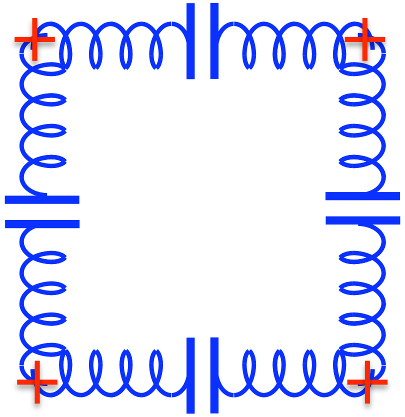

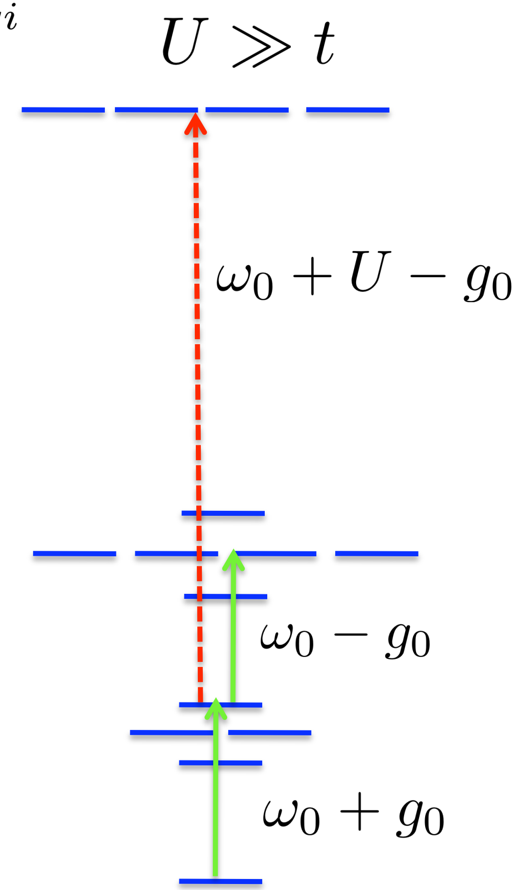

Strong interaction prohibits transitions to double occupancy, generate interesting state

$$(a_1^\dagger a_3^\dagger - a_2^\dagger a_4^\dagger)|g\rangle$$

State stable against varying U to U << t

$$(c_{k1}^\dagger c_{k3}^\dagger - c_{k2}^\dagger c_{k4}^\dagger)|g\rangle$$

Y. Hu, L Tian, in preparation (2009)

Superconducting Resonators

- Linear coupling to nanomechanical systems
- Quantum engineering and cooling of nanomechanical systems

Nanomechanical Resonator

1. Sometime ago
- Vibration of strings
- Dynamics – Euler-Bernoulli Eq.

2. Now, the decrease of size provides:
high frequency -- GHz
high Q – 10^{3-5} & $\Gamma = \omega_0/Q$

$$f_0 = \frac{(4.730)^2}{2\pi}\frac{1}{l^2}\sqrt{\frac{EI}{\rho A}}$$

E: Young Modulus
I: moment of inertia
ρ_a : linear density

3. quantum mechanics – (?) => **cooling**

$$H_v = \sum \frac{p_q^2}{2m} + \frac{m\omega_q^2 u_q^2}{2}$$

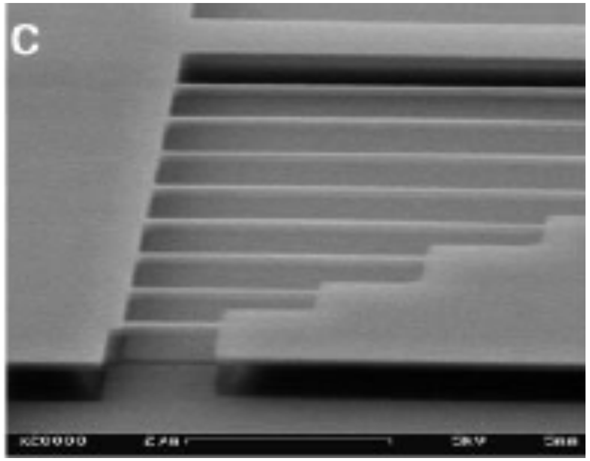

a doubly clamped beam, flexural modes

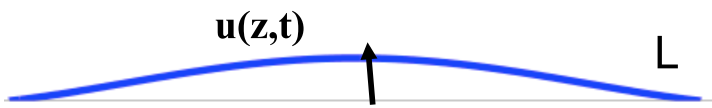

Can It Be Quantum Mechanical?

High quality factor over 10,000,000 (f=20 MHz) – Schwab, Harris …
very coherent once it becomes coherent
(calculation of Q-factor?)

Macroscopic quantum effects?
superconducting quantum tunneling
nanomechanical system - **cat state, entanglement** - test QM (?)

Barrier, thermal fluctuations T=24 mK=500 MHz
resonator frequency 10's kHz – GHz

$$n_{a0} = \frac{1}{e^{\hbar\omega/k_B T} - 1}$$

Why interesting?

- fundamental physics: quantum/classical boundary, using e.g. Schroedinger cat state
- metrology/calibration with resonators
- quantum data bus - ion trap
- continuous variable quantum information

Side Band Cooling Regime

Side band limit provides promise for ground state cooling
Recent experiments reach side band limit for NEMS - optical cavity and NEMS - superconducting resonator using optomechanical effects and NEMS - superconducting qubit
(Lehnert, Kippenberg, Wang, Schwab, Cleland/Martinis, Bouwmeester, Mavalvala, Chen ……),
Quantum regime is in visible future!

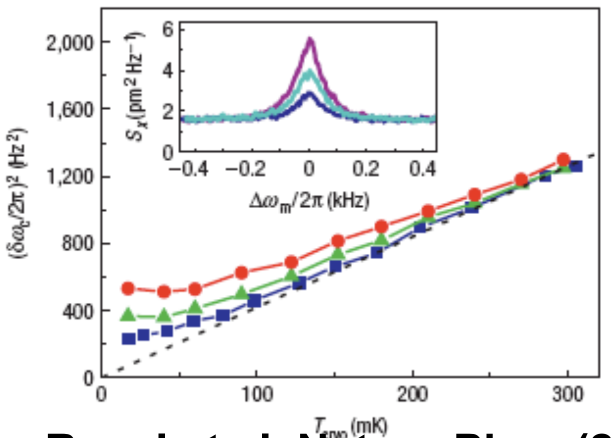

Regal et al, Nature Phys (2008)

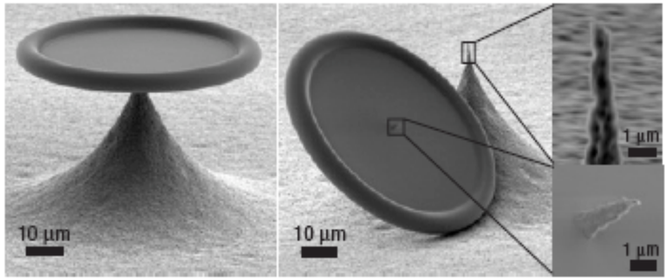

Schliesser et al, Nature Phys (2008)

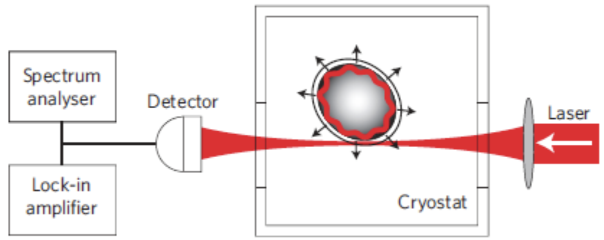

Park & Wang, Nature Phys (2009)

Nanomechanical System vs Solid-State Resonator

Josephson junction resonator

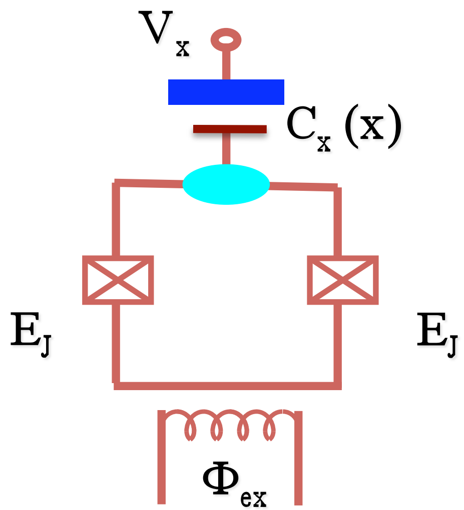

Transmission line resonator

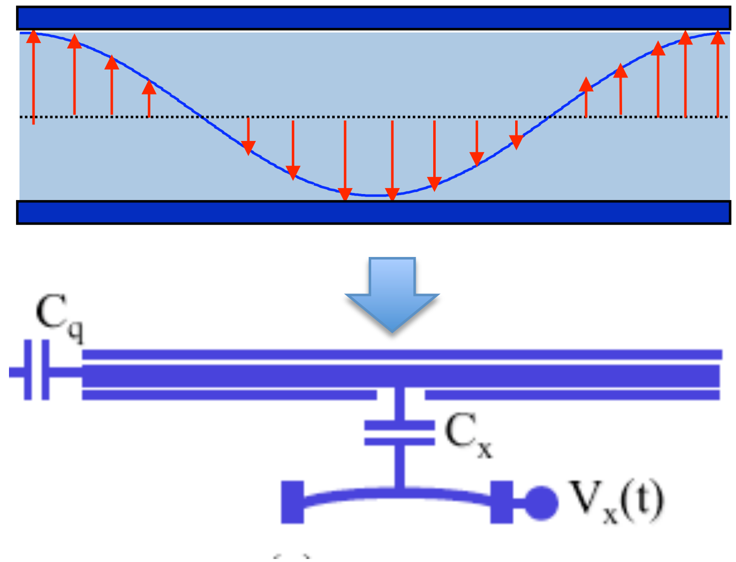

Capacitive coupling with solid-state resonators

- generate linear coupling $H_{int} = i\lambda(\hat{a} - \hat{a}^{\dagger})(\hat{b} + \hat{b}^{\dagger})\cos\omega_d t$
- frequency modulation by driving
- entanglement generated (two-mode squeezed vacuum state) $\exp(ra^2 - ra^{\dagger 2})|00\rangle$

Tian et al, NJP (2008)

Two Circuits for Mechanical Coupling

- Resonator capacitively coupling with mode Φ - LC oscillator
- Cooling from dynamic backaction

capacitance

$$C_x = C_{x0} + C'_x x$$

radiation pressure-like

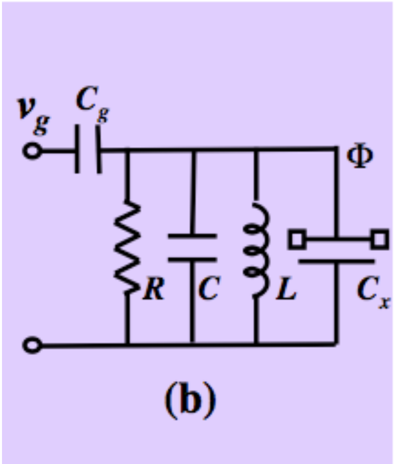

Previous scheme

parametrically modulated linear coupling

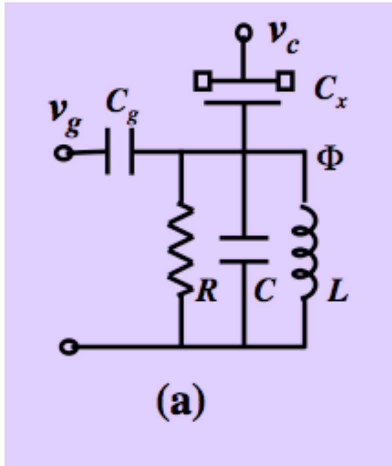

$$H_c = \hbar\omega_b b^\dagger b - g_r(a+a^\dagger)b^\dagger b$$

At typical parameters: $g_l \gg g_r$

Cooling: $v_c(t) = 2v_c \sin\omega_d t$

$$H_c = \hbar\omega_b b^\dagger b - g_r(a+a^\dagger)b^\dagger b - ig_l(a+a^\dagger)(b-b^\dagger)$$

$$g_r = (\hbar\omega_b/2)(C'_x \delta x_0/C_{\Sigma 0})$$

$$g_l = v_c\sqrt{\hbar\omega_b/2C_{\Sigma 0}}(C'_x \delta x_0)$$

Parametric Driving

- parametric driving provides "up-conversion" of low-energy mechanical quanta to high energy microwave photons, which then dissipate in circuit

- in rotating frame, effective energy for LC oscillator is $-\Delta$

$$H_t^{rot} = \hbar\omega_a a^\dagger a - \hbar\Delta b^\dagger b + g_l(a + a^\dagger)(b + b^\dagger)$$

- thermal bath has temp. T_0 with

$$n_{b0} = \frac{1}{e^{\hbar\omega_b / k_B T_0} - 1}$$

- effective temp. in rotating frame:

$$T_{eff} = T_0 \frac{|\Delta|}{\omega_b} \ll T_0$$

- "equilibrium" between thermal bath of mechanical mode and LC mode

Quantum Backaction Noise

Cooling of trapped ion at $-\Delta = \omega_b - \omega_d = \omega_a$

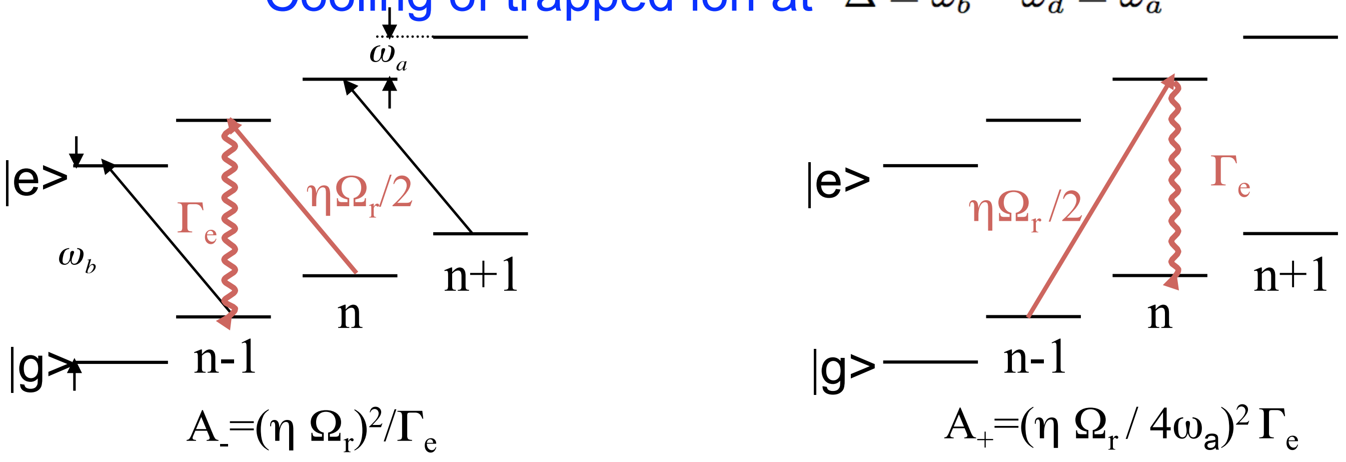

cooling circle

heating circle

<u>Our scheme is related to laser cooling scheme</u>

cooling transition $(a^\dagger b + b^\dagger a)$

cooling rate $A_- = 4g_l^2/(\hbar^2\kappa_0)$

heating transition $(a^\dagger b^\dagger + ba)$

heating rate $A_+ \approx g_l^2\kappa_0/(4\hbar^2\omega_a^2)$

$$g_l(a + a^\dagger)(b + b^\dagger)$$

$$v_c(t) = 2v_c \sin\omega_d t$$

- comparison
- also applies to n_0

$$n_0 = A_+/A_-$$

Backaction noise comes from counter rotating terms in the coupling

Cooling by Quantum Theory

<u>Quantum explanation - input-output theory</u>
operator equations can be solved in Heisenberg picture
<u>cooling rate</u> can be derived including self-energy
equation similar to <u>linearized equations for radiation pressure</u>

$$\Gamma_c = \frac{4(g_l/\hbar)^2\kappa_0|\Delta|\omega_a}{(\Delta^2-\omega_a^2+\frac{\kappa_0^2}{4})^2+\omega_a^2\kappa_0^2} = \frac{4g_l^2}{\hbar^2\kappa_0(1+\kappa_0^2/16\omega_a^2)}$$

red sideband

$$-\Delta = \omega_b - \omega_d = \omega_a$$

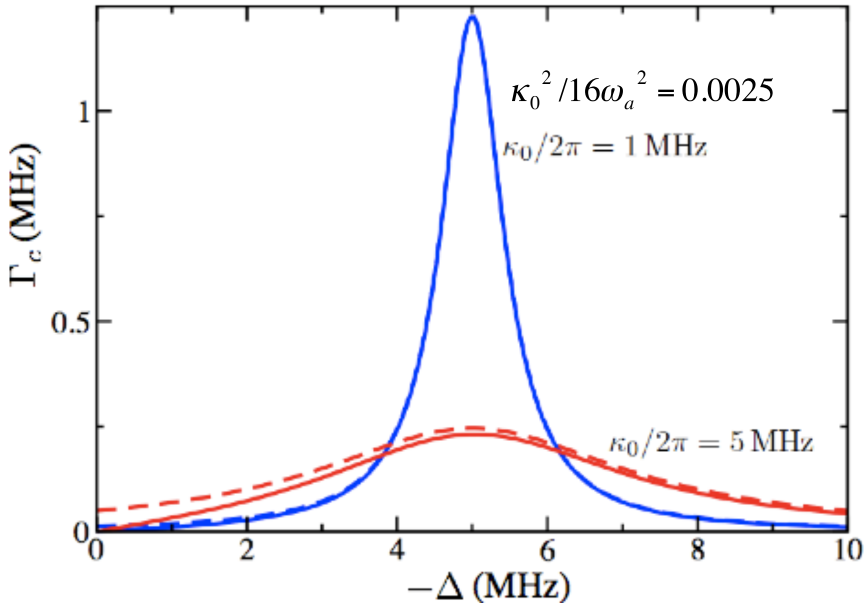

- solid - quantum theory
- dashed - semiclassical theory

maximal cooling at
(nearly) red sideband

Occupation Number

We calculated the n^f_a with no counter rotating terms: - P-representation

solid-lines: full quantum theory
dashed-lines: no counter rotating terms
$Q_m=\omega_a/\gamma_0$: quality factor of resonator

$$n_a^f = \frac{\Gamma_c n_0 + \gamma_0 n_{a0}}{\Gamma_c + \gamma_0} \approx n_0 + \frac{\gamma_0}{\Gamma_c} n_{a0}$$

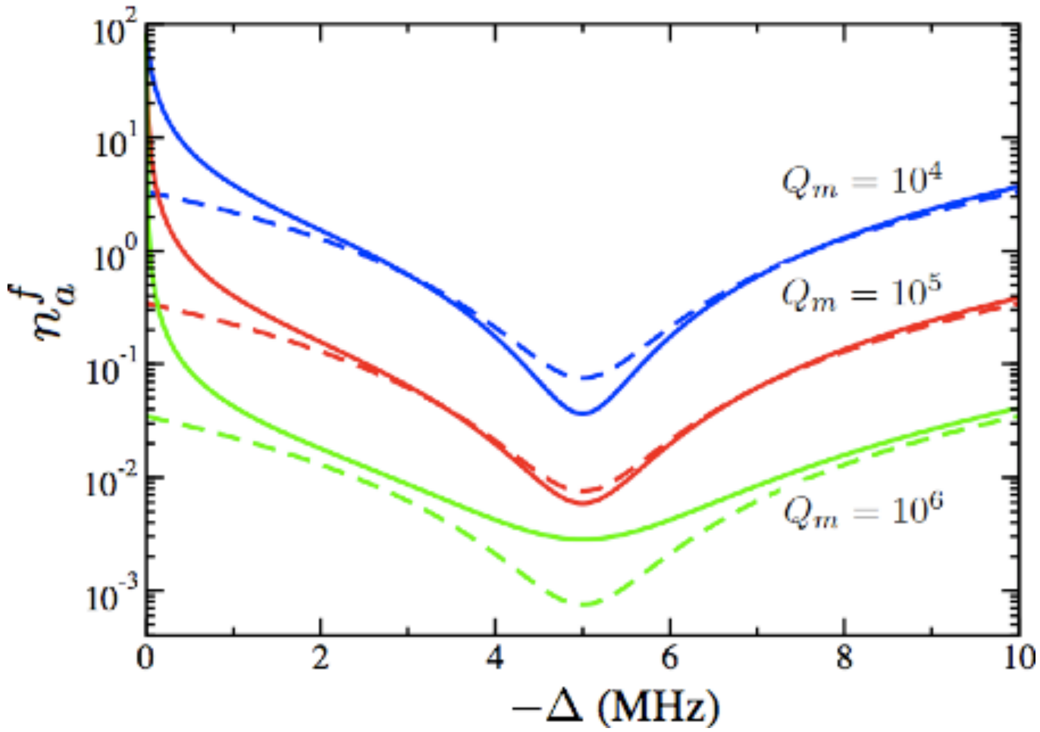

- low Q_m: 2nd term dominates
- high Q_m: backaction noise dominates, dashed curve can reach 0, solid curve reach n_0
- $Q_m=10^5$, $n_a^f=0.01<<1$

Tian, PRB (2009)

Parameters in Superconducting Circuits

Comparing with parameters in a few experiments, we choose the following:

	Ref [4, 5]	Ref [13]	Ref [14]	Our scheme	note
$\omega_b\,(2\pi\,\mathrm{GHz})$	5.2	–	–	7.5	LC oscillator frequency
$\kappa_0\,(2\pi\,\mathrm{MHz})$	.2	–	–	1	damping
Q	26,000	–	–	7,500	quality factor
$C_x\,(fF)$	.2	.13	.026	.2	coupling capacitance
$\partial C_x/\partial x\,(fF/\mu m)$	.2	2	.26	1	C_x'
$C_\Sigma\,(fF)$	–	1.3	.45	1.5	total capacitance
$\omega_a\,(2\pi\,\mathrm{MHz})$	1.5	117	19.7	5	mechanical frequency
n_{a0}	278	3.2	21	83.2	thermal occupation
$T_0\,(\mathrm{mK})$	20	20	20	20	possible temperature
$\gamma_m\,(2\pi\,\mathrm{kHz})$	.005	69	.56	.5	mechanical damping
Q_m	$>300,000$	1,700	35,000	10^4 - 10^6	mechanical quality factor
$mass\,(10^{-15}\mathrm{kg})$	6.2	2.84	.63	1.86	mass of resonator
$\delta x_0\,(fm)$	30	~ 5	26	30	quantum displacement
$d_0\,(\mathrm{nm})$	~ 1000	~ 65	~ 100	200	distance between capaciance plate
$v_c\,(\mathrm{mV})$	–	2500	–	< 300	gate voltage
$P\,(\mu W)$	< 1	–	–	.85	reactive power

Advantage – no need to pump the LC oscillator to high occupation

Conclusions

Solid-state devices provide a fruitful platform for quantum application

We discussed a few applications with superconductng resonators

- probling/copling TLS's – microscopic mechanism, TLS qubits
- coupling to qubit arrays – bistable behavior – interesting many-body state
- quantum engineering of entangled state …
- cooling to quantum limit of nanomechanical systems

More interesting questions to come ……

UC Merced – Campus